RESEARCH ARTICLE

A Critical Phenylalanine Residue in the Respiratory Syncytial Virus Fusion Protein Cytoplasmic Tail Mediates Assembly of Internal Viral Proteins into Viral Filaments and Particles

Fyza Y. Shaikh,[a] Reagan G. Cox,[a] Aaron W. Lifland,[b] Anne L. Hotard,[c] John V. Williams,[a,d] Martin L. Moore,[c] Philip J. Santangelo,[b] and James E. Crowe, Jr.[a,d,e]

Departments of Pathology, Microbiology and Immunology[a] and Pediatrics[d] and The Vanderbilt Vaccine Center,[e] Vanderbilt University Medical Center, Nashville, Tennessee, USA; Department of Pediatrics, Emory University and Children's Healthcare of Atlanta, Atlanta, Georgia, USA[c]; and Department of Biomedical Engineering, Georgia Institute of Technology and Emory University, Atlanta, Georgia, USA[b]

ABSTRACT **Respiratory syncytial virus (RSV) is a single-stranded RNA virus in the *Paramyxoviridae* family that assembles into filamentous structures at the apical surface of polarized epithelial cells. These filaments contain viral genomic RNA and structural proteins, including the fusion (F) protein, matrix (M) protein, nucleoprotein (N), and phosphoprotein (P), while excluding F-actin. It is known that the F protein cytoplasmic tail (FCT) is necessary for filament formation, but the mechanism by which the FCT mediates assembly into filaments is not clear. We hypothesized that the FCT is necessary for interactions with other viral proteins in order to form filaments. In order to test this idea, we expressed the F protein with cytoplasmic tail (CT) truncations or specific point mutations and determined the abilities of these variant F proteins to form filaments independent of viral infection when coexpressed with M, N, and P. Deletion of the terminal three FCT residues (amino acids Phe-Ser-Asn) or mutation of the Phe residue resulted in a loss of filament formation but did not affect F-protein expression or trafficking to the cell surface. Filament formation could be restored by addition of residues Phe-Ser-Asn to an FCT deletion mutant and was unaffected by mutations to Ser or Asn residues. Second, deletion of residues Phe-Ser-Asn or mutation of the Phe residue resulted in a loss of M, N, and P incorporation into virus-like particles. These data suggest that a C-terminal Phe residue in the FCT mediates assembly through incorporation of internal virion proteins into virus filaments at the cell surface.**

IMPORTANCE **Respiratory syncytial virus (RSV) is a leading cause of bronchiolitis and pneumonia in infants and the elderly worldwide. There is no licensed RSV vaccine and only limited therapeutics for use in infected patients. Many aspects of the RSV life cycle have been studied, but the mechanisms that drive RSV assembly at the cell surface are not well understood. This study provides evidence that a specific residue in the RSV fusion protein cytoplasmic tail coordinates assembly into viral filaments by mediating the incorporation of internal virion proteins. Understanding the mechanisms that drive RSV assembly could lead to targeted development of novel antiviral drugs. Moreover, since RSV exits infected cells in an ESCRT (endosomal sorting complexes required for transport)-independent manner, these studies may contribute new knowledge about a general strategy by which ESCRT-independent viruses mediate outward bud formation using viral protein-mediated mechanisms during assembly and budding.**

Received 29 December 2011 **Accepted** 5 January 2012 **Published** 7 February 2012

Citation Shaikh FY, et al. 2012. A critical phenylalanine residue in the respiratory syncytial virus fusion protein cytoplasmic tail mediates assembly of internal viral proteins into viral filaments and particles. mBio 3(1):e00270-11. doi:10.1128/mBio.00270-11.

Editor Anne Moscona, Weill Medical College, Cornell University

Address correspondence to James E. Crowe, Jr., james.crowe@vanderbilt.edu.

Respiratory syncytial virus (RSV) is a leading cause of serious viral lower respiratory tract illness in infants and the elderly worldwide. The virus is a member of the *Paramyxoviridae* family, and the genome consists of a single-stranded, negative-sense RNA molecule that encodes 11 proteins. The virion contains three glycoproteins: the fusion (F) protein, attachment glycoprotein (G), and small hydrophobic (SH) protein. The F protein is sufficient for mediating viral entry into cells *in vitro*. The G protein plays a role in viral attachment, and the SH protein is thought to inhibit apoptosis (1). RSV also contains six internal structural proteins: the matrix (M) protein, nucleoprotein (N), phosphoprotein (P), large (L) polymerase protein, and two isoforms of matrix protein 2 (M2-1 and M2-1). The M protein provides structure for the virus particle. RSV N, P, and L form the ribonucleoprotein (RNP) complex, which encapsidates the RSV genome and functions as the RNA-dependent RNA polymerase. M2-1 and M2-2 are accessory proteins that control transcription and replication (2).

Viral proteins traffic to the apical surface of polarized epithelial cells, where they assemble into virus filaments at the plasma membrane (3). However, the mechanisms that drive assembly into filaments and budding are not well understood. Generation of nascent RSV genomic RNA appears to occur in discrete cytoplasmic inclusion bodies that contain the RSV N, P, L, and M2-1 and -2 proteins but not the F, G, or SH protein (4). It is suspected that the

RNP complexes form in the inclusions and then traffic to the apical membrane, where they meet with the surface glycoproteins F, G, and SH arriving from the Golgi apparatus through the secretory pathway (5). RSV proteins and viral RNA assemble into virus filaments at the cell surface. These filaments are thought to contribute to cell-cell spread of the virus and morphologically resemble the filamentous form of virions seen in electron microscopy (EM) studies of virus produced in polarized cells (6). Live imaging has shown these structures to be dynamic, with rotation and directional movement (7, 8). Filament formation can also be modulated by alterations in the function of host proteins, including myosin Vb and Rab11a family interacting proteins 1 and 2. Budding occurs in a Vps-4-independent manner (6, 9), resulting in pleomorphic particles ranging from 150 to 250 nm in diameter for spherical forms and up to 10 μm long in filamentous forms (10).

Previously, we showed that the F protein traffics to the apical surface in the absence of any other viral protein or viral RNA and that the F-protein cytoplasmic tail (FCT) was completely dispensable for apical trafficking (5). It is unlikely, however, that a paramyxovirus would retain such a domain if it did not play some role in replication or pathogenesis, and indeed other investigators showed that a virus lacking the FCT had a 100- to 1,000-fold decrease in viral titers in a multicycle growth curve. This mutant virus was unable to form filaments at the cell surface but was capable of accomplishing cell-cell fusion (11, 12). Furthermore, the cytoplasmic tail (CT) of many paramyxovirus glycoproteins has been shown to be important for assembly and budding (11, 13).

Since the FCT is required for efficient replication but is not required for fusion or trafficking, we hypothesized that the FCT coordinates the assembly of viral proteins into filaments at the cell surface. In this study, we demonstrate that a key phenylalanine (Phe) residue in the FCT is critical for RSV assembly into filaments at the cell surface. Moreover, when Phe was mutated, RSV F was unable to recruit RSV M, N, and P efficiently into virus-like particles (VLPs). These studies indicate that the FCT, and specifically a Phe residue at amino position 22 of the FCT, is responsible for recruitment of internal viral proteins into filamentous structures at the cell surface for efficient assembly and subsequent budding.

RESULTS

RSV infection induced virus filaments that contain RSV F, M, N, and P. We first tested whether the cell surface filaments induced by RSV infection of epithelial cells contained all of the expected RSV structural proteins. HEp-2 cell monolayer cultures were inoculated with RSV wild-type (wt) strain A2 and incubated in complete growth medium for 24 h. The cell monolayers were then fixed and immunostained for the RSV F, M, N, or P protein or host cell filamentous actin (F-actin). In addition, we also stained cells for the presence of RSV genomic RNA using a fluorescently conjugated probe designed to hybridize to RSV gene start sequences (14). Figure 1 shows RSV filaments protruding from the cell membrane (A to P). Morphologically, these filaments often were clustered and kinked, and they stained brightly with antibodies to the RSV F protein. The filamentous structures contained RSV F, M, N, P, and viral RNA, indicating that both structural and genomic components are present. Thus, these filaments likely are virions assembling at the plasma membrane prior to budding.

Since RSV filaments might resemble host cell protrusions that contain cytoskeletal proteins, we next sought to distinguish viral filaments from cell projections simply decorated with the RSV F protein. Previous work in the field has shown that F-actin is not found in viral filaments (15). Therefore, we visualized F-actin using phalloidin to distinguish viral filaments from host structures containing F-actin (e.g., microvilli, filapodia, lamellipodia, and membrane ruffles). Figure 1Q to T show that viral filaments, marked by the presence of the RSV F protein, did not contain F-actin. Viral filaments also did not contain either tubulin or ezrin (data not shown). Although the viral and host filamentous structures often occurred in the same regions of the plasma membrane, viral filaments were distinct from the cell projections that contained cytoskeletal proteins. These data are consistent with previously published data that provide evidence for specific RSV protein sorting into viral filaments (6).

RSV virus-like filaments can be generated independent of viral infection. We next sought to determine the minimal requirements for RSV filament formation by transfecting combinations of plasmids encoding RSV proteins. Transfection of cDNAs encoding the RSV F, M, N, and P genes into HEp-2 cells induced formation of virus-like filaments that resembled viral filamentous structures formed during infection. Figure S1 in the supplemental material shows a representative image of filaments formed when these four RSV structural proteins were expressed in HEp-2 cells. Consistent with RSV filaments formed during infection, virus-like filaments contained RSV proteins and were often kinked, clustered, and stained brightly for the F protein (see Fig. S1A to D). RSV F was found to be necessary for virus-like filament formation (see Fig. S1E to H), and in fact, exclusion of any single gene of the four during transfection eliminated filament formation (data not shown). Thus, the filaments formed using the transfection-based assay were similar to filaments formed during viral infection in both morphology and composition. We used the transfection-based filament formation assay as a tractable system with which to study the role of the F protein CT domain in viral assembly at the plasma membrane.

RSV FCT terminal residues Phe-Ser-Asn are required for filament formation. We and others have shown that the FCT domain is not required for F-protein trafficking to the cell surface (5, 12). We asked here whether the CT domain was dispensable for viral assembly into filaments at the cell surface. We designed a panel of altered cDNAs of the F protein gene in which the CT domain was truncated or otherwise mutated (Fig. 2). We tested the effect of the tail mutations on virus-like filament formation at the cell surface using the transfection-based assay characterized in Fig. S1 in the supplemental material. When expressed alone, the F protein with wild-type cytoplasmic tail (FCT wt) did not form virus-like filaments and localized to cellular projections that contained F-actin (Fig. 3A to D). However, when coexpressed with M, N, and P, FCT wt was able to form virus-like filaments that were distinct from cellular projections containing F-actin (Fig. 3E to H). Therefore, we used the presence of F-actin as a marker to distinguish virus-like filaments from cellular projections, since only the latter contained F-actin. In contrast to FCT wt, deletion of the terminal 3 amino acids from the FCT (residues Phe-Ser-Asn, or FSN) resulted in a loss of virus-like filament formation and altered localization of the F protein only to F-actin-containing cellular protrusions (Fig. 3I to L). This pattern of altered F staining at the cell surface was similar to the pattern of FCT wt when it was expressed alone in HEp-2 cells (i.e., in the absence of the RSV N, P, and M proteins). Deletion of the three terminal amino acids of the

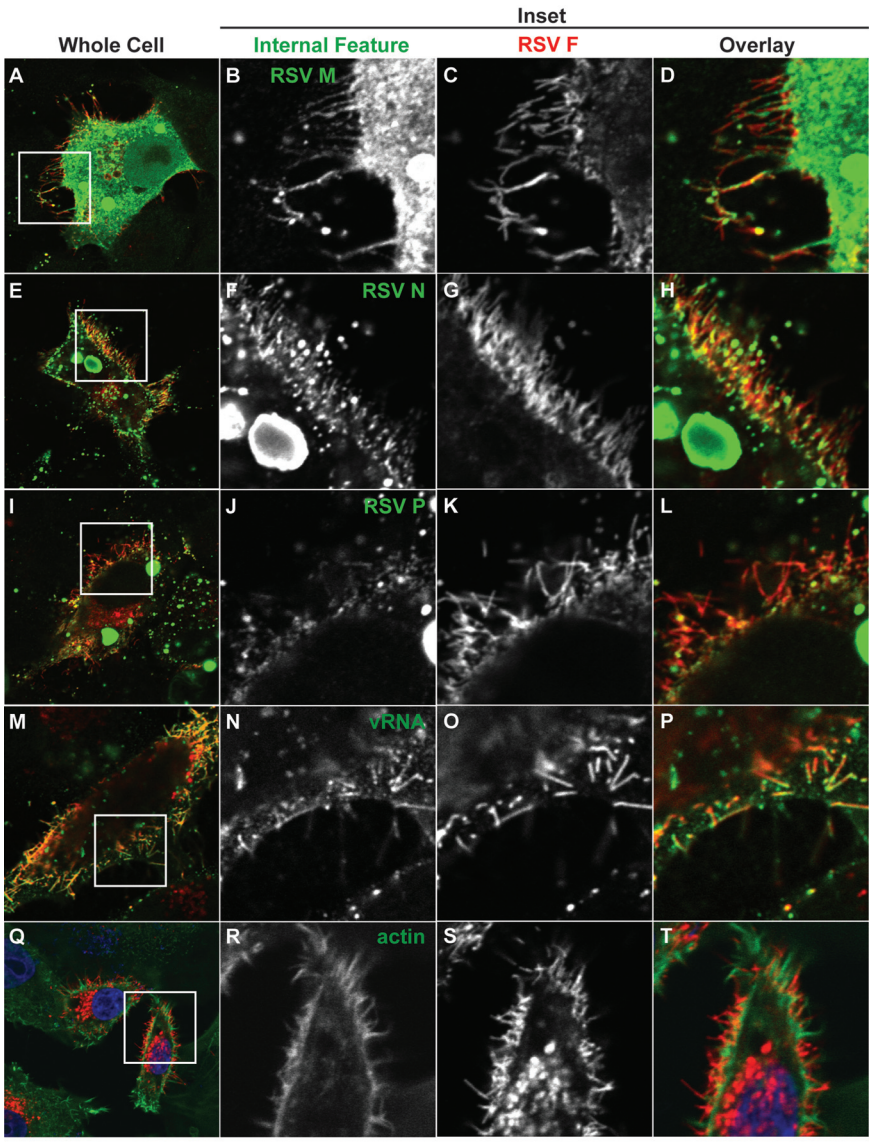

FIG 1 RSV F, M, N, P, and viral RNA localize to viral filaments during infection. HEp-2 cells were inoculated with RSV strain A2 at a MOI of 1.0 and incubated for 24 h. RSV F, M, N, and P were detected by indirect immunofluorescence; viral RNA (vRNA) was detected using an RNA probe specific to the RSV genomic gene start sequences; actin was detected using phalloidin. Column 1 (A, E, I, M, and Q) shows the entire cell. Panels B to D, F to H, J to L, N to P, and R to T show an enlargement of the inset shown in column 1. Column 2 (B, F, J, N, and R) shows RSV M, N, P, vRNA, or phalloidin staining only; column 3 (C, G, K, O, and S) shows RSV F only; and column 4 (D, H, L, P, and T) shows the overlay, with RSV F in red and RSV M, N, P, vRNA, or actin in green.

CT domain resulted in the same phenotype of F distribution as deletion of the entire tail domain (Fig. 3M to P). This FCT deletion construct was similar to the transmembrane-domain-plus-one-anchor-residue ("TM+1") construct that we previously described (5) and is designated FCTΔ23. For each truncation construct, total cellular expression and total surface expression of the F protein were measured at levels equivalent to those of FCT wt (Fig. 3M and N, respectively). Therefore, reduced expression or trafficking of the mutant protein to the cell surface did not play a role in the failure of these CT truncation constructs to form virus-like filaments. These data indicate that the terminal CT residues Phe-Ser-Asn are necessary for assembly of RSV proteins into virus-like filaments.

Phe-Ser-Asn residues are sufficient for viral protein assembly into filaments at the cell surface. Based on the data presented in Fig. 3, we next sought to determine if the specific residues Phe-Ser-Asn on the C terminus of FCT were necessary for filament formation when coexpressed with M, N, and P or alternatively if only the 24-amino-acid length of the CT domain determined filament formation. We mutated all three terminal residues to alanines (FCTΔ3 AAA) in order to test the hypothesis that a CT of a certain length was necessary for viral assembly. FCTΔ3 AAA was impaired for virus-like filament formation when coexpressed with RSV M, N, and P (Fig. 4E to H) compared to results for FCT wt (Fig. 4A to D). In order to determine if residues Phe-Ser-Asn were sufficient for virus-like filament formation, we deleted the entire FCT except for the terminal residues Phe-Ser-Asn (designated FΔCT FSN). FΔCT FSN formed virus-like filaments at the cell surface (Fig. 4I to L) that were similar in length to FCT wt filaments (Fig. 4M), but the percentage of transfected cells with filaments was reduced 10-fold (Fig. 4N). These data suggest that other residues in the CT or a minimum length of the CT may be important for initiation of filament formation. The total cellular expression and total surface expression of FCTΔ3 AAA or FΔCT FSN were similar to those of FCT wt, again indicating that neither expression nor trafficking to the cell surface was impaired (Fig. 4O and P, respectively). These data suggest that residues Phe-Ser-Asn are necessary and sufficient for assembly of viral structural proteins into virus-like filaments at the cell surface.

The Phe residue in the RSV FCT is necessary for filament formation. In order to determine if a particular residue of the FCT Phe-Ser-Asn motif was the determining factor for viral assembly into filaments, we designed FCT constructs that contained mutations of each of the three terminal residues individually. We compared the abilities of the mutant FCT constructs to form virus-like filaments when coexpressed with M, N, and P to that of FCT wt (Fig. 5A to D). When the Phe residue was mutated to an alanine (F22A), virus-like filaments failed to form, and the F construct colocalized with cellular structures containing F-actin (Fig. 5E to H). However, if either the Ser or Asn residue was mutated to an alanine, the mutant FCT constructs were able to assemble into virus-like filaments, distinct from cellular structures containing F-actin (Fig. 5I to L and 5M to P, respectively). Total cellular

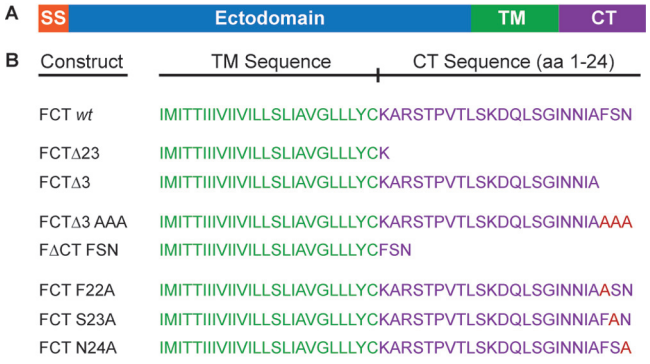

FIG 2 Schematic of FCT constructs. (A) FCT mutant constructs were generated using site-directed mutagenesis from FCT wt in the pcDNA3.1 vector. Functional regions are indicated by color: SS, signal sequence (orange); ectodomain (blue); TM, transmembrane domain (green); CT, cytoplasmic domain (purple). (B) Sequences of the TM and CT domain are indicated for each construct. Point mutations are indicated in red. We designated residue K as FCT residue 1. The schematic is not to scale.

expression and total surface expression of each of the FCT constructs with single amino acid mutations were equivalent to FCT wt levels, indicating that neither expression nor trafficking was impaired (Fig. 5Q and R, respectively). We also designed and tested FCT constructs with conservative mutations (F22Y, S23T, and N24Q). The results were similar to the data described for the alanine point mutations in Fig. 5 (data not shown). Collectively, these data show that the Phe residue near the C-terminal end of FCT plays a key role in filamentous viral assembly at the plasma membrane.

The Phe residue is required for incorporation of RSV M, N, and P into RSV VLPs. Next, we sought to determine why the FCT Phe residue was necessary for virus assembly into filaments. We first introduced the FCTΔ3 mutation into a recombinant virus using a plasmid-based virus rescue system, but this mutant virus could not be rescued, likely due to the drastic effect on assembly. We then developed a VLP assay to determine whether the FCT Phe

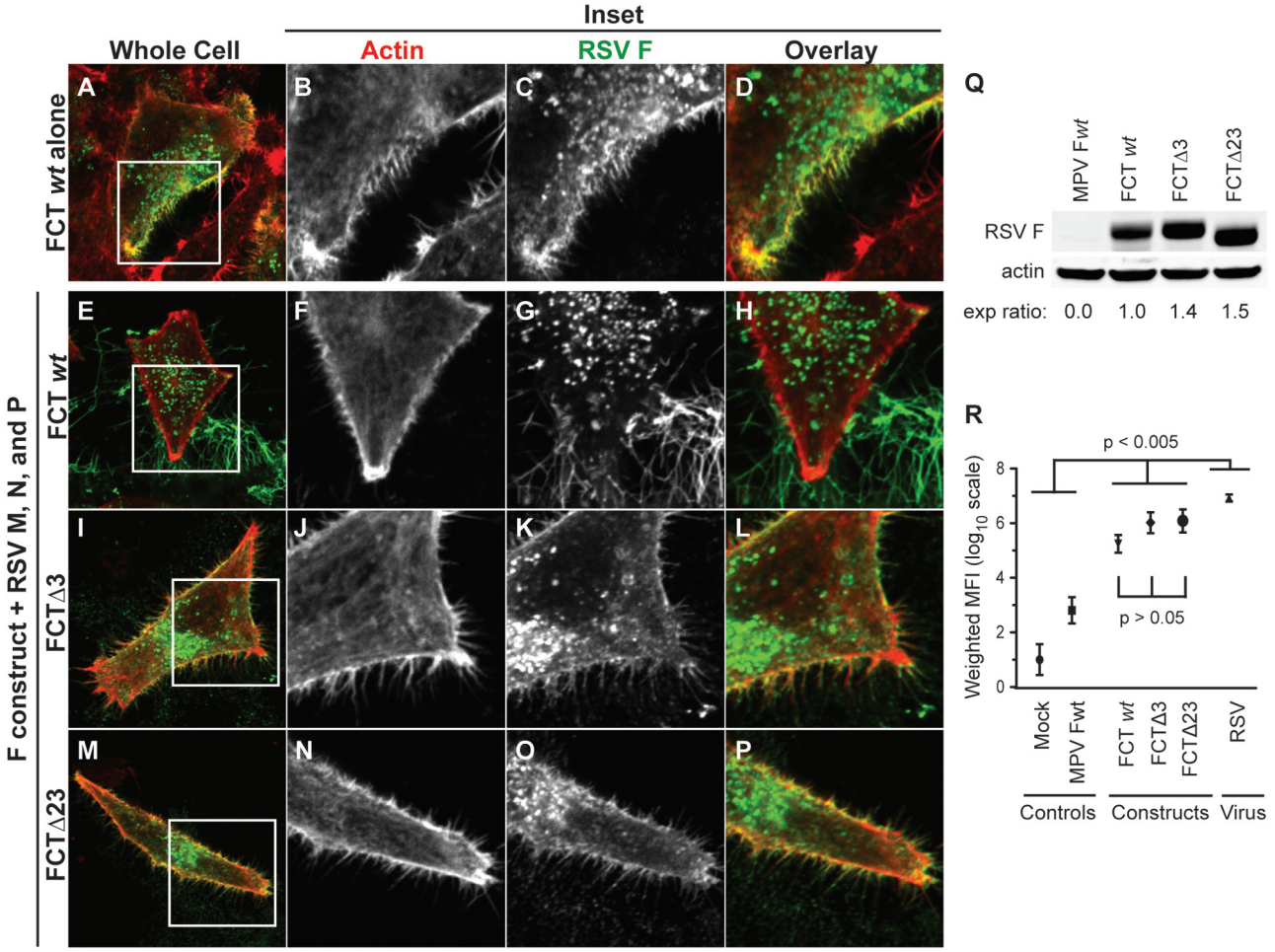

FIG 3 **FCT** terminal residues Phe-Ser-Asn are required for filamentous assembly at the cell surface. HEp-2 cells were transfected with FCT wt only (A to D) or with the indicated FCT construct and plasmids encoding RSV M, N, and P (E-P). Column 1 shows images of the whole cell (A, E, I, and M). Columns 2 to 4 (B to D, F to H, J to L, and N to P) show an enlargement of the corresponding inset in column 1. Column 2 shows actin staining only (B, F, J, and N); column 3 shows RSV F staining only (C, G, K, and O); and column 4 shows the overlay, with actin in red and RSV F in green (D, H, L, and P). (Q) Total cell lysate was collected from HEp-2 cells transfected with the indicated FCT construct, and RSV F or actin was detected by immunoblotting. The RSV F band was normalized against actin, and the expression (exp) ratio represents a normalization to results for FCT wt. (R) Total surface expression of RSV F was determined by flow cytometry using HEp-2 cells transfected with the indicated FCT construct and RSV M, N, and P. Data are plotted as means, and error bars represent standard deviations. Weighted MFI is mean fluorescence intensity (MFI) × the frequency of positive cells. MPV F wt is used as a specificity control.

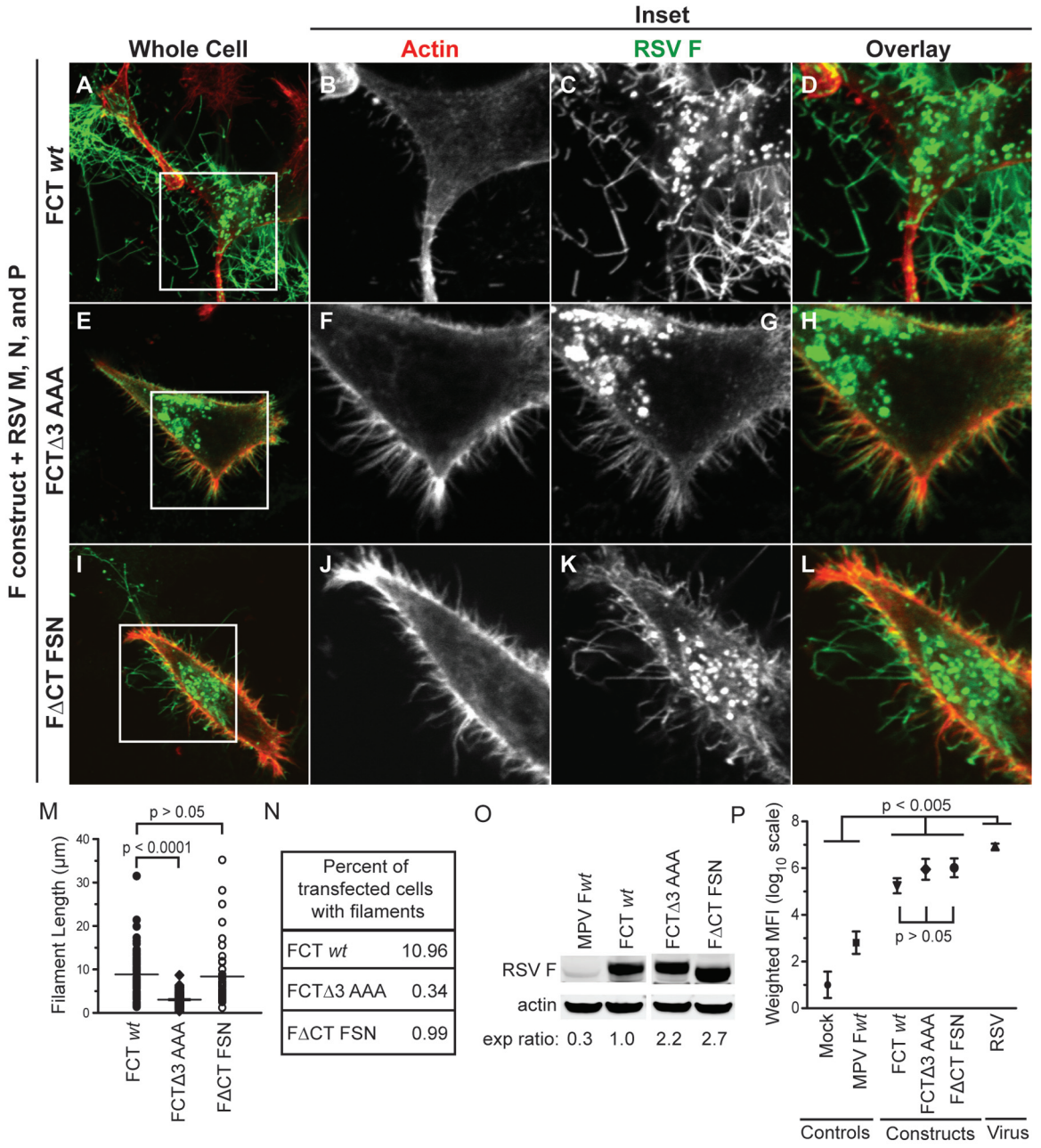

FIG 4 FCT residues Phe-Ser-Asn are sufficient for filamentous assembly at the cell surface. HEp-2 cells were transfected with the indicated FCT construct and RSV M, N, and P (A to L). Column 1 shows images of the whole cell (A, E, and I). Columns 2 to 4 (B to D, F to H, and J to L) show an enlargement of the corresponding inset in column 1. Column 2 shows actin staining only (B, F, and J); column 3 shows RSV F staining only (C, G, and K); and column 4 shows the overlay, with RSV F in green and actin in red (D, H, and L). (M and N) HEp-2 cells were transfected as described for panels A to L. Filament length was determined by measuring the lengths of individual filaments using Zeiss LSM software as described in Materials and Methods (M). Percent transfected cells was determined by counting RSV F-transfected cells with filaments and then dividing that number by the total number of RSV F-transfected cells (N). (O) Total cell lysate was collected from HEp-2 cells transfected with the indicated FCT construct, and RSV F and actin were detected by immunoblotting. The RSV F band was normalized against actin, and the expression (exp) ratio represents a normalization to FCT wt. (P) Total surface expression of RSV F was determined by flow cytometry using HEp-2 cells transfected with the indicated FCT construct and RSV M, N, and P. Data are plotted as means, and error bars represent standard deviations. Weighted MFI is mean fluorescence intensity (MFI) × the frequency of positive cells. MPV F wt is used as a specificity control.

residue determined the ability of the F protein to assemble internal virion proteins into VLPs. 293-F cells were used for their high growth rate, dense cell growth, and transfection efficiency, all of which have been limiting factors in previous efforts to develop VLP assays with conventional transformed epithelial cells lines, such as HEp-2 cells (data not shown). Using this system, sufficient VLPs were produced for relative protein quantification by immunoblotting using the Lycor Odyssey infrared imaging system. Second, previous work in the field has shown that F, M, N, and P are the minimal requirements for passage of a minigenome construct

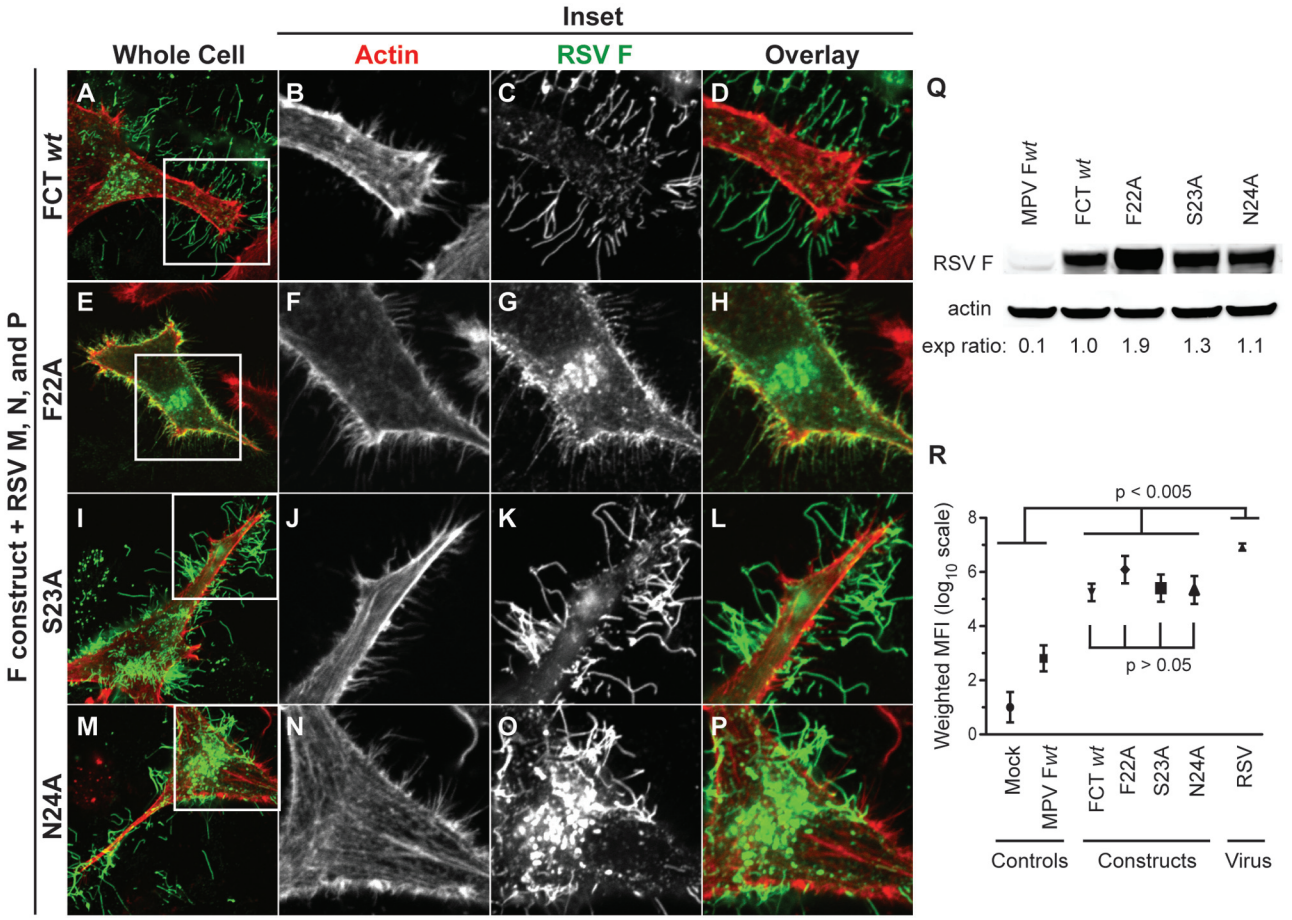

FIG 5 The Phe residue at position 22 in the RSV FCT is necessary for filamentous assembly at the cell surface. HEp-2 cells were transfected with the indicated FCT construct and RSV M, N, and P (A to P). Column 1 shows images of the whole cell (A, E, I, and M). Columns 2 to 4 (B to D, F to H, J to L, and N to P) show an enlargement of the corresponding inset in column 1. Column 2 shows actin staining only (B, F, J, and N); column 3 shows RSV F staining only (C, G, K, and O); and column 4 shows the overlay, with RSV F in green and actin in red (D, H, L, and P). (Q) Total cell lysate was collected from HEp-2 cells transfected with the indicated FCT construct, and RSV F or actin were detected by immunoblotting. The RSV F band was normalized against actin, and the expression (exp) ratio represents a normalization to FCT wt. (R) Total surface expression of RSV F was determined by flow cytometry using HEp-2 cells transfected with the indicated FCT construct and RSV M, N, and P. Data are plotted as means, and error bars represent standard deviations. Weighted MFI is mean fluorescence intensity (MFI) × the frequency of positive cells. MPV F wt is used as a specificity control.

consisting of the RSV leader and trailer sequences flanking a reporter gene (16). Since we found that these proteins are also the minimum requirements for filament formation independent of viral infection, we choose to express VLPs using all four proteins to recapitulate the minimum requirements for assembly and budding.

RSV VLPs were produced by transfecting cells with plasmids encoding the indicated F construct and wt M, N, and P. TEM analysis of VLPs showed characteristic F-protein spikes (black arrows) on the surface of particles similar to those seen on RSV virion particles produced and imaged in the same manner (Fig. 6A and B). Second, the diameter of the VLPs was similar to that of RSV and within the usual range of diameter of virions grown in other cell types (10). In addition to structure, we also compared the protein composition of VLPs with that of virus. Figure 6C shows a representative immunoblot comparing the level of each viral protein in the VLPs to that in virions. These data were quantified from three independent experiments and are presented as percentages of RSV virion protein levels (Fig. 6D). Compared to virus, the VLPs contained equivalent amounts of the F protein but less M, N, and P. Although the ratios of the F protein to internal proteins differed between VLPs and RSV, VLPs did still incorporate RSV internal proteins, thus allowing us to study the relative abilities of various FCT constructs to incorporate internal virion proteins into budded vesicles. Several possibilities could explain the discrepancy of ratios. The VLPs may incorporate a higher proportion of F into each particle than M, N, and P, compared to those for virions, or there may be vesicles containing the F protein alone escaping into the supernatant. We favor the latter, since transfection of cDNA encoding the F protein alone led to a baseline transport of F into the supernatant (data not shown).

After initial validation of the VLP system, we sought to determine how the FCT Phe residue affected VLP budding and the incorporation of internal virion proteins. We performed the VLP assay as described above and collected the cell pellets for total protein expression. Figure 6E shows immunoblots from a representative experiment. Data were normalized to the

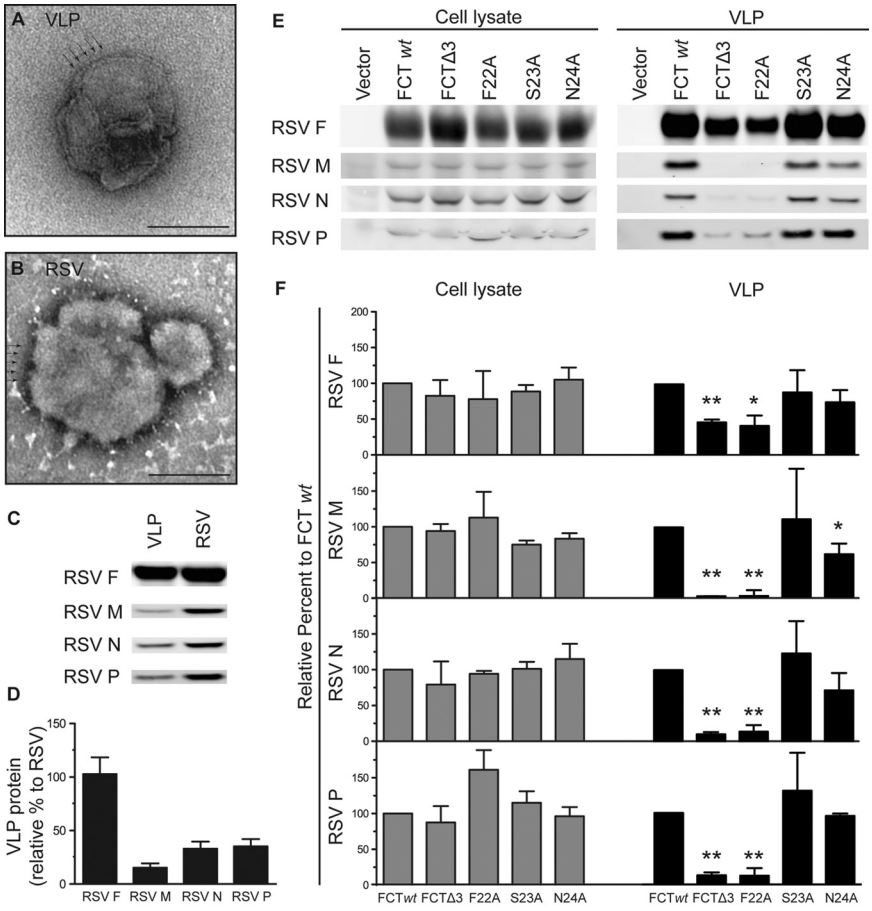

FIG 6 The Phe residue at position 22 in the RSV FCT is necessary for incorporation of internal virion proteins into VLPs. 293-F cells were transfected with plasmids encoding RSV FCT wt, M, N, and P or infected with RSV at an MOI of 0.05. Panels A and B show transmission electron micrographs of a representative VLP and virion, respectively. Scale bars represent 100 nm. (C to D) Supernatants from RSV-infected or FCT wt-transfected cells were clarified and pelleted through a 20% sucrose cushion. Panel C shows a representative blot comparing protein levels in VLPs to RSV. Panel D shows a quantification of three independent experiments as shown in panel C. The indicated protein levels in VLPs were normalized to that of the corresponding protein in RSV. For panels E and F, 293-F cells were transfected with plasmids encoding the indicated FCT construct and RSV M, N, and P. Panel E shows a representative experiment with indicated protein levels in cell lysates (left) or VLPs (right). Panel F shows a quantification of data from three independent experiments as shown in panel E (cell lysates in grey; VLPs in black). Data are plotted as means, and error bars represent standard deviations.

levels in the FCT wt sample, and the means and standard deviations from three independent experiments are shown in Fig. 6F. Compared to FCT wt, when residues Phe-Ser-Asn were deleted (FCTΔ3) or Phe was mutated to an alanine (F22A), there was a significant loss of RSV M, N, and P protein incorporation into VLPs. In contrast, point mutations of residue Ser or Asn (S23A or N24A, respectively) did not affect incorporation of RSV M, N, or P into VLPs. The FCTΔ3 and F22A constructs also induced less transfer of the F protein into the supernatant than the FCT wt, S23A, or N24A constructs, consistent with less budding of VLPs. These data show that the Phe residue in the FCT is necessary for RSV M, N, and P incorporation into VLPs. Collectively, the data in this report show that the FCT mediates viral assembly through a C-terminal Phe residue in order to incorporate RSV M, N, and P into virus filaments at the cell surface prior to budding.

DISCUSSION

The RSV FCT domain is known to play a critical role in viral replication, but the mechanism by which the FCT functions in assembly and budding has not been well characterized. In this study, we determined that a single critical Phe residue in the FCT at amino acid position 22 mediates assembly of virus-like filaments, incorporation of RSV internal proteins into VLPs, and subsequent budding of VLPs from cells. The finding that a single amino acid residue in the FCT can control both assembly and budding is remarkable. We studied the role of RSV proteins in assembly of filaments independent of viral infection by expressing proteins from plasmids, and we found that filament formation requires the F, M, N, and P proteins. This assembly process likely is driven by interactions of these viral proteins with each other or collectively with host proteins. Using cDNA-based expression of F proteins with alterations in the FCT, we determined the key residue in the FCT that is required for assembly of virus-like filaments containing the four minimally required structural proteins, F, M, N, and P. Furthermore, we used a VLP budding assay under the same protein expression conditions to reveal that the FCT coordinates assembly through its ability to incorporate M, N, and P into particles. These data provide a direct link between FCT coordination of viral assembly into filaments and budding of viral particles. Alternatively, the formation of filaments and virus particles may be two different outcomes of essentially the same assembly process, with the Phe residue serving in a critical role for both processes.

The specific mechanisms that govern FCT-mediated assembly, however, are still not well defined. Our data show that expression, trafficking, and surface expression of F are not affected by mutations in the FCT. This finding is consistent with findings of previous studies that indicated the TM domain of F is responsible for targeting the protein to the apical surface (5), and localization to specific lipid microdomains in the plasma membrane appears to depend on an unidentified domain in the ectodomain (17). Therefore, it is likely that the FCT Phe residue we identified is critical for a protein-protein interaction. A simple explanation may be that this residue directly interacts with one of the internal virion proteins, such as M, N, or P, or a complex of these proteins. On the other hand, the F protein is a trimer, and the FCT is located in close proximity to the plasma membrane. It may be that the hydrophobic Phe residue confers a specific conformation to the cytoplasmic portion of the trimer. Finally, the possibility of an interaction with a host

protein or complex of proteins cannot be excluded. Future studies will focus on elucidating the specific protein-protein interactions mediated by the FCT and how these interactions lead to the incorporation of other viral proteins into filaments.

Coordination of RSV assembly by the FCT would be consistent with findings of many other studies citing paramyxovirus glycoprotein cytoplasmic tails as crucial to both assembly and budding (13). For RSV and human metapneumovirus (HMPV), members of the *Pneumovirus* subfamily, the G protein is dispensable for viral replication *in vitro* (18, 19). Although the FCT may be sufficient, optimal incorporation of viral proteins and RNA might require both F and G since residues in the RSV G protein CT are thought to be important for interactions with M (20). However, for the *Paramyxoviridae* subfamily, the requirement of glycoprotein CTs varies with each virus. For measles virus and Sendai virus assembly, the F protein CT is required. Newcastle disease virus F and HN glycoproteins interact with different internal viral proteins, M and N, respectively. In contrast, the F and HN CTs of parainfluenza virus 5 serve somewhat redundant functions (13). The lack of a common theme for the role of CT domains in paramyxoviruses may simply indicate that many questions about the specific mechanisms of viral assembly remain unanswered, and further investigation into the RSV FCT may contribute to general knowledge regarding glycoprotein CT-mediated assembly for other paramyxoviruses.

In addition to viral protein incorporation, the structural formation of RSV particles at the cell surface also requires viral interactions with the host cell lipid membrane. The viral particle membrane first must be deformed outward as an extension of the cell membrane. Then, the particle must be elongated by incorporation of additional membrane to create long filaments. Finally, a scission event must occur to release the viral particle from the cell membrane. All of these processes are energy intensive and require complex coordination of surface proteins and nucleocapsids containing RNA and viral proteins (21). Many viruses usurp endosomal sorting complexes required for transport (ESCRT) machinery to accomplish the task of outward bud formation and membrane scission using late domains found in viral proteins (13). Viral budding using late domains requires the AAA ATPase Vps4. However, inhibition of Vps4 does not affect RSV budding (6), and like other ESCRT-independent viruses, RSV may use viral protein-mediated pushing and pulling forces to initiate membrane bending at lipid microdomains in order to exit the cell (21). RSV has been shown to assemble into filaments at lipid microdomains (22, 23). The RSV F protein has been shown to associate with detergent-resistant membranes (DRMs), as have the RSV M, N, P, M2-1, and L proteins during viral infection (17, 23–25). Furthermore, the M protein associates with lipid microdomains in the presence of the F protein (26). Our data suggest that the Phe residue in the FCT is critical for F-protein interactions with internal virion proteins in order to provide both the pulling and pushing forces needed to bend the membrane in order to form filaments, presumably at lipid microdomains. Our data also provide some insight about how the FCT mediates initial membrane bending and filament elongation. The ability of a shortened CT with only residues Phe-Ser-Asn to form virus-like filaments was reduced by 10-fold. However, once this was initiated, the shortened CT was able to induce filaments that elongated to lengths comparable to those generated by FCT wt. These data suggest that other residues or a minimum length of the CT may be important for initiation of outward bud formation.

Manipulation of the plasma membrane also likely involves a variety of host proteins that function at the cell surface. Many cellular structures extending outward from the cell surface depend on actin polymerization (e.g., microvilli, filapodia, lamellipodia, and membrane ruffles), and lipid microdomains have been linked to the cortical actin network (27). In fact, disruption of actin-associated signaling pathways has been shown to affect filament formation, and β-actin and actin-related proteins have been found in the same sucrose gradient-purified fractions as RSV (15, 28–32). However, actin polymerization has been shown to be dispensable for filament formation, and F-actin is excluded from viral filaments (15). While actin and actin-related proteins likely are involved in aspects of RSV assembly, our data support the hypothesis that the process by which viral proteins extend the cell membrane outward to form filaments is distinct from the process used by actin-based cellular structures. Exclusion of cellular proteins from viral filaments also argues for specific sorting of viral and host proteins into filaments, a process that likely is highly regulated and involves interactions among viral proteins, host proteins, and lipid microdomains.

Despite these studies, the mechanism by which RSV assembles and buds is still incompletely defined. Viral protein-protein and protein-lipid interactions likely play a significant role, and further investigation will yield insight into what motifs mediate these interactions for both viral and cellular glycoproteins. Further study of RSV assembly and budding will contribute to general understanding of how ESCRT pathway-independent viruses can exit the cell and how viral surface and internal proteins contribute to egress. Finally, understanding the mechanisms that drive RSV assembly and budding could lead to targeted development of novel antiviral drugs for prophylactic or therapeutic use against RSV infection.

MATERIALS AND METHODS

Cell culture and wt RSV virus preparations. HEp-2 cells (ATCC CCL-23) were maintained in Opti-MEM I medium (Invitrogen) containing 2% (vol/vol) fetal bovine serum (FBS), 1% (vol/vol) l-glutamine, 2.5 μg/ml amphotericin B, and 1% (vol/vol) penicillin-streptomycin. Suspension 293-F cells were maintained as recommended by the manufacturer (Freestyle 293 expression system; Invitrogen). Transfections were performed using the Effectene transfection reagent (Qiagen) for HEp-2 cells and the Polyfect transfection reagent (Qiagen) for 293-F cells. The RSV wt strain A2 was expanded in HEp-2 cells.

RSV infections. For filament visualization, HEp-2 cell monolayers on 12-mm micro-cover glasses (no. 2; VWR) were inoculated at a multiplicity of infection (MOI) of 1.0 and incubated for 24 h. For flow cytometric analysis, HEp-2 cells in tissue culture flasks were inoculated at an MOI of 3.0 and incubated for 24 h. For the virus-like particle (VLP) assay, 293-F cells were infected at an MOI of 0.05 for 72 h.

Generation of RSV F protein mutant constructs. All DNAs encoding the RSV fusion (F) protein constructs in this study were made from a sequence-optimized cDNA encoding the RSV wt strain A2 F protein in the pcDNA3.1 plasmid vector (Invitrogen) (5). DNAs encoding RSV F proteins with truncations or other alterations of the cytoplasmic tail at the C terminus of the protein were cloned using PCR primers to amplify the desired length of the tail and subcloned into pcDNA3.1. Targeted mutations, insertions, or deletions were introduced using the Lightning site-directed mutagenesis kit (Stratagene) and confirmed by sequencing.

Filament formation. Plasmids encoding the wt or a mutant RSV F protein along with pcDNA3.1 plasmids containing inserts encoding the

RSV A2 strain matrix (M), nucleoprotein (N), and phosphoprotein (P) gene (synthesized by GeneArt, Regensburg, Germany) were transfected into HEp-2 cell culture monolayers using 0.2 μg of each plasmid DNA, and cells were incubated for 72 h. Cells were fixed, immunostained, and imaged as described below. All images for virus-like filament formation were collected in a single experiment using identical microscopy parameters.

Fixation and immunostaining. Cells were fixed with 3.7% (wt/vol) paraformaldehyde in phosphate-buffered saline (PBS) for 10 min. Cells were permeabilized with 0.3% (wt/vol) Triton X-100 and 3.7% paraformaldehyde in PBS for 10 min at room temperature (RT). After fixation, cells were blocked in 3% (wt/vol) bovine serum albumin (BSA) in PBS for 60 min, followed by addition of primary antibody (Ab) in the blocking solution for 60 min. Cells were then washed three times in PBS, and species-specific IgG Alexa Fluor (Invitrogen) was added at a dilution of 1:1,000 in block solution for 60 min to detect primary Abs. Cells were washed three times in PBS and fixed on glass slides using the Prolong Antifade kit (Invitrogen). All steps were performed at RT. Images were obtained on a Zeiss inverted LSM510 confocal microscope using a 63×/1.40 Plan-Apochromat oil lens. Anti-RSV M (clone B135), anti-RSV P protein (clone 3_5), and anti-RSV N protein (clone B130) monoclonal Abs were a kind gift of Earling Norrby and Ewa Bjorling. An anti-RSV F protein humanized mouse monoclonal Ab (palivizumab; MedImmune) was obtained from the Vanderbilt Pharmacy. F-actin was visualized using rhodamine phalloidin, and To-Pro-3 iodide was used to visualize the nucleus (Invitrogen).

Imaging with RSV-specific RNA probe and live cell delivery. Single-copy sensitive RNA probes designed to target the RSV genomic gene start regions were delivered into RSV wt- or mock-infected HEp-2 cells using streptolysin O reversible permeabilization 24 h after inoculation, as previously described (14). After probe delivery, cells were immunostained for RSV proteins as described above. Images were processed in Volocity imaging software (version 5.1; Improvision). Shadow and highlight input sliders were adjusted to the beginning and end of the histogram curve to optimize tonal levels for the entire image; middle tones were not adjusted.

Quantitative analysis of images. To determine filament length, images from 12 high-powered fields were obtained on a Zeiss inverted LSM510 confocal microscope using a 40×/1.30 Plan-Neofluar oil lens. Images were analyzed using laser scanning microscopy (LSM) image acquisition software (Rel 4.2; Zeiss). The length of virus-like filaments was determined using the ruler tool in the LSM software to trace individual filaments in the images. The four longest filaments measured per cell were used in calculation of overall filament length for each construct. For quantitation of the percentage of RSV F-transfected cells showing filaments, images from 20 high-powered fields were collected on a Zeiss inverted LSM510 confocal microscope using a 20×/0.75 Plan-Apochromat lens. The percentage of RSV F-transfected cells with filaments was calculated by counting the total number of RSV F-transfected cells with filaments and dividing that number by the total number of RSV F-transfected cells.

Quantitative analysis of total cell lysate. HEp-2 cells in 6-well plates were transfected with 0.4 μg of plasmid DNA encoding the indicated F-protein cytoplasmic tail (CT) construct using the Qiagen Effectene transfection reagent. Cells were harvested at 48 h after transfection using a single detergent lysis buffer (50 mM Tris-HCl, 150 mM NaCl, 1% Triton X-100, pH 8.0) containing a 1:200 dilution of mammalian protease inhibitor cocktail (Sigma). Lysates were separated on 4 to 12% NuPAGE bis-Tris gels and transferred to polyvinylidene difluoride (PVDF) membranes using an iBlot dry blotting system (Invitrogen). Membranes were blocked for 1 h using Odyssey blocking buffer (Li-Cor) diluted 1:1 in PBS. Primary Abs for β-actin (1:5,000; Abcam) or the RSV F protein (motavizumab expressed from recombinant cDNA; 0.85 μg/ml) were diluted in blocking buffer diluted 1:1 with PBS + 0.1% Tween 20 (PBS-T), applied to membranes, and incubated overnight at 4°C. Membranes then were washed four times in PBS + 0.1% Tween for 5 min each. Secondary Abs were diluted 1:2,500 (goat anti-human IRDye 680CW; Kirkegaard & Perry Labs Inc.) or 1:5,000 (goat anti-mouse IRDye 800CW; Li-Cor) in blocking buffer and added to each membrane for 60 min. Membranes were washed four times in PBS-T. Bands were imaged and quantitated using the Odyssey infrared imaging system. The quantitative signals from RSV F protein bands were normalized against those of β-actin in the same lane and used to generate an expression (exp) ratio that represented a comparison of expression of the mutant F protein to that of the wt F protein.

Flow cytometric assay for quantitative surface expression of RSV F. HEp-2 cells on 6-well plates were transfected with 0.4 μg of each plasmid encoding the wt RSV M, N, and P proteins and either RSV F wt or a mutant F construct using the Effectene transfection reagent (Qiagen). After 48 h, cells were treated with 20 mM EDTA in PBS to form a single-cell suspension. Cells were washed two times in wash buffer (2% FBS in PBS) and then incubated with palivizumab at 1 μg/ml for 30 min at RT. Cell were again washed two times with wash buffer and immunostained with an Alexa Fluor goat anti-mouse 488 secondary Ab at a final concentration of 2 μg/ml. Cells were washed two times in wash buffer and analyzed on a 5-laser custom LSR II flow cytometer (Becton Dickinson) in the Vanderbilt Medical Center Flow Cytometry Shared Resource. Data analysis was performed using the FlowJo software program (version 7.6.1). Weighted mean fluorescent intensity (MFI) was calculated by multiplying the raw mean fluorescent intensity by the frequency of positive cells. All flow cytometry data from Fig. 3, 4, and 5 were collected using the same negative and positive control samples in three independent experiments. Statistical analysis was performed using a Student's *t* test. *P* values less than 0.05 were considered significant.

VLP assay. A recent protocol developed for the generation of human metapneumovirus VLPs (R. G. Cox and J. V. Williams, unpublished results) was modified for the preparation of RSV VLPs. 293-F cells were transfected with plasmids encoding either vector alone or RSV M, N, P, and the indicated RSV F construct in equal amounts. Seventy-two hours after transfection, cell supernatants and pellets were separated and collected by using low-speed centrifugation. Cell pellets were resuspended in cell lysis buffer as described above. Cell supernatant was pelleted through a 20% sucrose cushion using a Sorvall Surespin 630 rotor at 26,000 rpm for 90 min. The resulting pellet was resuspended in equal volumes of cell lysis buffer with protease inhibitors (Sigma). Western blotting was performed as described above. The quantitative signals from RSV F, M, N, or P protein bands were corrected for background using vector alone and then normalized to the signal from wt FCT. Bars represent the means and standard deviations for three independent experiments. Statistical analysis was performed using Student's *t* test. All values less than 0.05 were considered significant.

Transmission electron microscopy. VLP transfections were prepared as described for the VLP assay with FCT wt. For RSV-infected samples, 293-F cells were inoculated at an MOI of 0.05 for 72 h. Cell supernatants were clarified and pelleted though 20% sucrose in sterile MHN buffer (0.1 M $MgSO_4$, 50 mM HEPES, 150 mM NaCl). Pellets were resuspended in 20% sucrose in MHN, applied to formvar-carbon grids with 300 mesh Cu (Ted Pella Inc.), and stained with 1% aqueous sodium phosphotungstate acid (Electron Microscopy Sciences). Grids were imaged on a FEI Morgagni electron microscope operated at an acceleration voltage of 100 kV. Images were collected using a 1,000 × 1,000 active pixel charge-coupled-device (CCD) camera (AMT) at a magnification of ×44,000. Image contrast was enhanced in the Adobe Photoshop (CS5) software program using the levels adjustment. Shadow and highlight input sliders were adjusted to the beginning and end of the histogram curve to optimize tonal levels for the entire image; middle tones were not adjusted.

ACKNOWLEDGMENTS

This work was supported by the Vanderbilt Medical Scientist Training Program National Institute of General Medical Sciences/NIH grant T32 GM007347, Burroughs Wellcome Fund Clinical Scientist Award in Translation Research (to J.E.C.), a grant from the March of Dimes (J.E.C.), and NIH grants R01 GM 094198 (to P.J.S.) and R01 AI85062 (to J.V.W.). Experiments were performed in part through the VUMC Cell

Imaging Shared Resources (supported by NIH grants CA68485, DK20593, DK58404, HD15052, DK59637, and EY08126) and the VMC Flow Cytometry Shared Resource (supported by the Vanderbilt Ingram Cancer Center [P30 CA68485] and the Vanderbilt Digestive Disease Research Center [DK058404]).

We thank Melanie Ohi, Thuy Tran, and Kim Crimin for equipment use and expertise with data collection and analysis. We thank all members of the Crowe Laboratory, especially Natalie Thornburg, for helpful discussion and excellent technical support.

SUPPLEMENTAL MATERIAL

Supplemental material for this article may be found at http://mbio.asm.org/lookup/suppl/doi:10.1128/mBio.00270-11/-/DCSupplemental.

Figure S1, PDF file, 0.3 MB.

REFERENCES

1. **Fuentes S, Tran KC, Luthra P, Teng MN, He B.** 2007. Function of the respiratory syncytial virus small hydrophobic protein. J. Virol. **81**: 8361–8366.
2. **Fields BN, Knipe DM, Howley PM.** 2007. Fields virology, 5th ed. Wolters Kluwer Health/Lippincott Williams & Wilkins, Philadelphia, PA.
3. **Roberts SR, Compans RW, Wertz GW.** 1995. Respiratory syncytial virus matures at the apical surfaces of polarized epithelial cells. J. Virol. **69**: 2667–2673.
4. **Lindquist ME, Lifland AW, Utley TJ, Santangelo PJ, Crowe JE, Jr.** 2010. Respiratory syncytial virus induces host RNA stress granules to facilitate viral replication. J. Virol. **84**:12274–12284.
5. **Brock SC, Heck JM, McGraw PA, Crowe JE, Jr.** 2005. The transmembrane domain of the respiratory syncytial virus F protein is an orientation-independent apical plasma membrane sorting sequence. J. Virol. **79**: 12528–12535.
6. **Utley TJ, et al.** 2008. Respiratory syncytial virus uses a Vps4-independent budding mechanism controlled by Rab11-FIP2. Proc. Natl. Acad. Sci. U. S. A. **105**:10209–10214.
7. **Bächi T.** 1988. Direct observation of the budding and fusion of an enveloped virus by video microscopy of viable cells. J. Cell Biol. **107**:1689–1695.
8. **Santangelo PJ, Bao G.** 2007. Dynamics of filamentous viral RNPs prior to egress. Nucleic Acids Res. **35**:3602–3611.
9. **Brock SC, Goldenring JR, Crowe JE, Jr.** 2003. Apical recycling systems regulate directional budding of respiratory syncytial virus from polarized epithelial cells. Proc. Natl. Acad. Sci. U. S. A. **100**:15143–15148.
10. **Bächi T, Howe C.** 1973. Morphogenesis and ultrastructure of respiratory syncytial virus. J. Virol. **12**:1173–1180.
11. **Branigan PJ, et al.** 2006. The cytoplasmic domain of the F protein of human respiratory syncytial virus is not required for cell fusion. J. Gen. Virol. **87**:395–398.
12. **Oomens AG, Bevis KP, Wertz GW.** 2006. The cytoplasmic tail of the human respiratory syncytial virus F protein plays critical roles in cellular localization of the F protein and infectious progeny production. J. Virol. **80**:10465–10477.
13. **Harrison MS, Sakaguchi T, Schmitt AP.** 2010. Paramyxovirus assembly and budding: building particles that transmit infections. Int. J. Biochem. Cell Biol. **42**:1416–1429.
14. **Santangelo PJ, et al.** 2009. Single molecule-sensitive probes for imaging RNA in live cells. Nat. Methods **6**:347–349.
15. **Jeffree CE, et al.** 2007. Ultrastructural analysis of the interaction between F-actin and respiratory syncytial virus during virus assembly. Virology **369**:309–323.
16. **Teng MN, Collins PL.** 1998. Identification of the respiratory syncytial virus proteins required for formation and passage of helper-dependent infectious particles. J. Virol. **72**:5707–5716.
17. **Fleming EH, Kolokoltsov AA, Davey RA, Nichols JE, Roberts NJ, Jr.** 2006. Respiratory syncytial virus F envelope protein associates with lipid rafts without a requirement for other virus proteins. J. Virol. **80**: 12160–12170.
18. **Biacchesi S, et al.** 2004. Recombinant human metapneumovirus lacking the small hydrophobic SH and/or attachment G glycoprotein: deletion of G yields a promising vaccine candidate. J. Virol. **78**:12877–12887.
19. **Teng MN, Whitehead SS, Collins PL.** 2001. Contribution of the respiratory syncytial virus G glycoprotein and its secreted and membrane-bound forms to virus replication *in vitro* and *in vivo*. Virology **289**: 283–296.
20. **Ghildyal R, et al.** 2005. Interaction between the respiratory syncytial virus G glycoprotein cytoplasmic domain and the matrix protein. J. Gen. Virol. **86**:1879–1884.
21. **Chen BJ, Lamb RA.** 2008. Mechanisms for enveloped virus budding: can some viruses do without an ESCRT? Virology **372**:221–232.
22. **Brown G, et al.** 2004. Analysis of the interaction between respiratory syncytial virus and lipid-rafts in Hep2 cells during infection. Virology **327**:175–185.
23. **McCurdy LH, Graham BS.** 2003. Role of plasma membrane lipid microdomains in respiratory syncytial virus filament formation. J. Virol. **77**:1747–1756.
24. **Marty A, Meanger J, Mills J, Shields B, Ghildyal R.** 2004. Association of matrix protein of respiratory syncytial virus with the host cell membrane of infected cells. Arch. Virol. **149**:199–210.
25. **McDonald TP, Pitt AR, Brown G, Rixon HW, Sugrue RJ.** 2004. Evidence that the respiratory syncytial virus polymerase complex associates with lipid rafts in virus-infected cells: a proteomic analysis. Virology **330**: 147–157.
26. **Henderson G, Murray J, Yeo RP.** 2002. Sorting of the respiratory syncytial virus matrix protein into detergent-resistant structures is dependent on cell-surface expression of the glycoproteins. Virology **300**:244–254.
27. **Lillemeier BF, Pfeiffer JR, Surviladze Z, Wilson BS, Davis MM.** 2006. Plasma membrane-associated proteins are clustered into islands attached to the cytoskeleton. Proc. Natl. Acad. Sci. U. S. A. **103**:18992–18997.
28. **Burke E, Dupuy L, Wall C, Barik S.** 1998. Role of cellular actin in the gene expression and morphogenesis of human respiratory syncytial virus. Virology **252**:137–148.
29. **Fernie BF, Gerin JL.** 1982. Immunochemical identification of viral and nonviral proteins of the respiratory syncytial virus virion. Infect. Immun. **37**:243–249.
30. **Gower TL, et al.** 2005. RhoA signaling is required for respiratory syncytial virus-induced syncytium formation and filamentous virion morphology. J. Virol. **79**:5326–5336.
31. **Radhakrishnan A, et al.** 2010. Protein analysis of purified respiratory syncytial virus particles reveals an important role for heat shock protein 90 in virus particle assembly. Mol. Cell. Proteomics **9**:1829–1848.
32. **Ulloa L, Serra R, Asenjo A, Villanueva N.** 1998. Interactions between cellular actin and human respiratory syncytial virus (HRSV). Virus Res. **53**:13–25.